Title

# Development and validation of a prediction model based on the organ-based metabolic tumor volume on FDG-PET in patients with differentiated thyroid carcinoma

Authors

Yuko Uchiyama, MD,[1,2] Kenji Hirata, MD, PhD,[1,2,*] Shiro Watanabe, MD, PhD,[1,2] Shozo Okamoto, MD, PhD,[3] Tohru Shiga, MD, PhD,[4] Kazufumi Okada, MPH,[5] Yoichi M. Ito, PhD,[5] Kohsuke Kudo, MD, PhD[1,6,7]

[1]Department of Diagnostic Imaging, Hokkaido University Graduate School of Medicine, Sapporo, Japan

[2]Department of Nuclear Medicine, Hokkaido University Hospital, Sapporo, Japan

[3]Department of Radiology, Obihiro-Kosei General Hospital, Obihiro, Japan

[4]Advanced Clinical Research Center, Fukushima Global Medical Science Center, Fukushima, Japan

[5]Biostatistics Division, Clinical Research and Medical Innovation Center, Hokkaido University Hospital, Sapporo, Japan

[6]Department of Diagnostic Imaging and Interventional Radiology, Hokkaido University Hospital, Sapporo, Japan

[7]Global Center for Biomedical Science and Engineering, Faculty of Medicine, Hokkaido University, Sapporo, Japan

**First author:** Yuko Uchiyama, MD, PhD candidate, Department of Diagnostic Imaging, Graduate School of Medicine, Hokkaido University, Kita 15, Nishi 7, Kita-Ku, Sapporo, Hokkaido 060-8638, Japan. Tel.: +81-11-706-7779, Fax: +81-11-706-7408
Email: y_uchiyama@med.hokudai.ac.jp

***Corresponding author:** Dr. Kenji Hirata, Department of Diagnostic Imaging, Graduate School of Medicine, Hokkaido University, Kita 15, Nishi 7, Kita-Ku, Sapporo, Hokkaido 060-8638, Japan.
Tel.: +81-11-706-7779, Fax: +81-11-706-7408
Email: khirata@med.hokudai.ac.jp

**Source of Funding:**
This work was supported by a grant from the JSPS KAKENHI, no. JP20K08015.

**Running Title:** Organ-based MTV in thyroid cancer

**Total word count:** 4081

Total number of figures: 5
Total number of tables: 3

## ABSTRACT

**Background:** Although patients with differentiated thyroid cancer (DTC) generally have a good prognosis, patients with a large metabolic tumor volume (MTV) on FDG-PET may experience poor clinical courses. We measured organ-based MTVs and tested its prognostic performance in comparison to conventional MTV (cMTV).

**Methods:** We retrospectively analyzed the cases of 280 patients who received their first I-131 therapy in 2003–2014 at our hospital and showed an FDG-avid metastatic lesion. We randomly divided the patients into training (n=190) and validation (n=90) datasets. We classified the MTVs as $MTV_{neck\text{-}node}$, $MTV_{distant\text{-}node}$, $MTV_{lung}$, $MTV_{bone}$, and $MTV_{other\text{-}organs}$ and tested with/without dichotomization vis-à-vis overall survival (OS). Based on the estimated weighting coefficients of the organ-based MTVs, we propose a new index: the adjusted whole-body MTV (aMTV). Using the validation dataset, we compared the aMTV with cMTV for predicting OS.

**Results**: In a univariate analysis, $MTV_{distant\text{-}node}$ and $MTV_{other\text{-}organs}$ were more strongly correlated with the OS than the dichotomized forms, whereas the dichotomized forms of $MTV_{neck\text{-}node}$, $MTV_{lung}$, and $MTV_{bone}$ were more strongly correlated with OS than the continuous variables. The aMTV was thus expressed as $0.69 \times dic(MTV_{neck\text{-}node}) + 0.02 \times MTV_{distant\text{-}node} + 1.05 \times dic(MTV_{lung}) + 1.58 \times dic(MTV_{bone}) + 0.01 \times MTV_{other\text{-}organs}$, where dic(x) represents 0 or 1 based on the optimized cut-off. In the model evaluation using the validation group, aMTV was a significant predictor of OS with a higher c-index (0.7676) than cMTV (0.7218).

**Conclusion**: In DTC patients with FDG-avid metastasis before I-131 therapy, all organ-based MTVs were significant predictors of prognosis. As the aMTV outperformed the cMTV for predicting prognoses, we recommend measuring the MTV on an organ basis.

**Key words**

differentiated thyroid carcinoma, metabolic tumor volume, organ-based measurement, FDG-PET

## Introduction

Patients with differentiated thyroid cancer (DTC) have a relatively good prognosis with slow progress in most cases, but there is a group of DTC patients who experience a poor clinical course. The known clinical factors associated with poor prognosis in DTC include a large primary lesion, advanced patient age at the first diagnosis, male sex, and the presence of metastasis [1, 2]. F-18 fluorodeoxyglucose (FDG) positron emission tomography (PET) is a useful clinical tool to predict the prognosis of DTC patients, as in other malignancies. It has been clarified those patients with FDG-avid metastasis had worse prognoses than those without FDG-avid metastasis [3, 4].

Metabolic tumor volume (MTV) and total lesion glycolysis (TLG) derived from FDG-PET/CT have been reported to be good prognostic factors for various malignant tumors [5–7]. There have also been reports that a higher MTV and TLG in FDG-PET are factors associated with poor prognosis in DTC [8, 9]. However, it has been indicated that in cases of DTC, the neck lymph nodes have little effect on the patients' overall survival (OS) [10], and that the prognosis is poor when the patient has distant metastasis in organs that are not commonly targets of metastasis, such as the liver and brain [11, 12]. These lines of evidence suggest that, even if their MTV values are equal, metastatic lesions that have developed at different organs may have different clinical impacts. Nevertheless, most of the investigations of the MTV and TLG have considered all metastatic lesions equally, i.e., the whole-body MTV calculated as the sum of the individual lesions' MTVs throughout the body is most commonly used. We hypothesized that both MTV measurements obtained in an organ-by-organ manner and the organ-adjusted whole-body MTV, defined as the weighted sum of the organ-based MTVs, may have better prognostic performance.

In this retrospective study, we aimed to develop an organ-based MTV-based model and to determine whether it is more useful for predicting the prognosis of patients with DTC compared to the conventional MTV.

## Subjects and Methods

*Subjects*

Based on the Transparent Reporting of Multivariate Prediction Model for Individual Prognosis or Diagnosis (TRIPOD) statement, the present study is categorized as type 2a [13]. This retrospective analysis was approved by our hospital's institutional review board (approval no. 020-0315). The requirement of written informed consent from each patient was waived because of the study's retrospective nature. We reviewed our hospital's information system to extract the cases of patients who underwent FDG-PET or PET/CT at our hospital before undergoing I-131 radioactive iodine therapy (RAI) for DTC between January 2003 and December 2014.

Based on the results of a computer-based search of the hospital's medical records, a total of 1,218 RAI treatments for 800 patients were performed for DTC during that period. Among them, 767 RAI treatments were identified as the first RAI after total thyroidectomy, and 33 RAI treatments were performed as the second or later RAI. Among the 767 cases of first RAI treatments, 425 patients proved to have one or more residual metastatic lesions in an examination before their RAI (details are provided below in the *Visual assessment of FDG-PET* section). Of these 425 patients, 290 showed any FDG-avid metastatic lesion in any organs; 10 of the patients were excluded as we could not access their clinical data. A final total of 280 patients (187 females [67%], 93 males [23%]) were enrolled (Fig. 1).

The mean ± SD patient age was 60.4 ± 13.5 years (range 13–84 years; median 64,

interquartile range [IQR]: 54–69 years). The data on patient survival during the follow-up period after FDG-PET were collected through routine clinical visits and telephone interviews. The follow-up period ranged from 1.13 to 154.8 months (median 54.5, IQR: 26.5–94.1 months). No patients were treated by a tyrosine kinase inhibitor (TKI) within the observation period.

*Image acquisition*

After 6-hr fasting and blood glucose measurement, the patient was injected with FDG (4.5 MBq/kg), followed by whole-body scanning 1 hr after the injection. Three different PET or PET-CT scanners were used in this cohort: (1) an ECAT EXACT HR+ PET scanner (Siemens, Munich, Germany) (n=14 patients), (2) an ECAT EXACT 47 PET scanners (Siemens) (n=128), and (3) a Biograph 64 PET/CT scanner (Siemens) (n=138).

For the ECAT EXACT HR+ and ECAT EXACT 47 PET scanners, 2-min emission scanning and 2-min transmission scanning with a 68Ge/68Ga source per bed position were performed, followed by image reconstruction using ordered subset expectation maximization (OSEM, 1 iteration, 30 subsets). For the Biograph 64 PET/CT scanner, low-dose CT images were acquired for attenuation correction, followed by 3-min emission scanning for each bed position. PET images were reconstructed using the TrueX algorithm, which is a point spread function implemented in OSEM (two iterations, 21 subsets). After reconstruction, the matrix sizes were 128×128 for both ECAT scanners and 168×168 for the Biograph64, and the voxel sizes were 3.4×3.4×3.4 mm for both ECAT scanners and 4.1×4.1×2.0 mm for the Biograph64.

*Visual assessment of FDG-PET*

The accumulation of FDG was visually evaluated and discussed by two board-certificated

nuclear medicine physicians (Y.U. and K.H., 18 years and 15 years of experience, respectively) to determine each patient's inclusion in this study. To evaluate the presence/absence of metastasis and metastatic organs, we collected each patient's serum thyroglobulin (sTg) level and findings from imaging examinations such as computed tomography (CT), magnetic resonance imaging (MRI), and ultrasonography (US) taken essentially within 1 month before RAI treatment, and the I-131 scintigraphy after the patient's initial therapy. The lesion was judged to be an FDG-avid metastatic lesion if it exhibited FDG uptake greater than that of the surrounding tissues.

*Semi-quantitative analysis*

For the image analysis, we used a free software package, Metavol [14]. First, any uptake masses with a standardized uptake value (SUV) ≥3.0 were automatically extracted. Then, the nuclear medicine physician with 18 years' experience categorized each uptake mass into 'tumor uptake' or 'non-tumor uptake.' In cases in which the tumor and non-tumor masses were connected, the non-tumor parts were carefully removed with the use of a manual region-of-interest tool. The same physician then categorized each tumor uptake by the organs.

We defined the organ-based MTV as the tumor volume at each organ, including neck node(s) ($MTV_{neck\text{-}node}$), distant node(s) ($MTV_{distant\text{-}node}$, i.e., lymph nodes beyond the neck), lung ($MTV_{lung}$), bone ($MTV_{bone}$), and other organs ($MTV_{other\text{-}organs}$). The 'other organs' included the liver (n=3), pleura (n=5), muscle (n=1), and kidney (n=1). A representative case is illustrated in Fig. 2.

*Statistical analyses*

The statistical analyses were performed using JMP Pro 14 and SAS 9.4 (SAS Institute Inc., Cary,

NC, USA) in the following three steps after we randomly divided all 280 patients into two groups (training, n=190; validation, n=90). The randomization was performed using Microsoft Excel. In the analyses described next, the training dataset was used in (i), (ii), and (iii), and the validation dataset was used in (iii).

i) Univariate analysis

We first performed a univariate analysis to test the prognostic value of each organ-based MTV. The Cox proportional hazard model was used to input the organ-based MTV as the single explanatory variable and to output the patients' overall survival (OS) as a response variable. We exhaustively searched for the best cut-off value to dichotomize each organ-based MTV. The cut-off value was adjusted by 0.1 mL until the dichotomized form of the organ-based MTV became the most prognostic (i.e., showed the highest c-index). The continuous form or the dichotomized form of each organ-based MTV, whichever was observed to be more predictive, was used for the subsequent analyses.

ii) Multivariate analysis (multivariate model construction)

We then constructed a Cox proportional hazard model to input the five organ-based MTVs to predict OS. The estimated regression coefficients were used as the weighting coefficients for a score calculation.

iii) Model validation

The constructed model was evaluated using the validation dataset. Using the weighting coefficients that were determined as described above, we defined the weighted sum of the five

organ-based MTVs as the 'adjusted whole-body MTV' (aMTV). For comparison, the simple sum of the organ-based MTVs was defined as the 'conventional MTV' (cMTV). Both the aMTV and cMTV were tested by a univariate Cox regression proportional hazard model with the OS as a dependent variable.

The patients' OS was analyzed by the Kaplan-Meier method with the log-rank test. For the univariate and multivariate analyses, p-values <0.05 were accepted as significant. The data of the patient groups in the Results section are presented as the range (median, IQR).

We also determined the time-dependent receiver operating characteristic (ROC) curve and area under the curve (AUC) of the ROC for the patients' 1-year, 3-year, and 5-year survival in both the training and validation datasets to evaluate the prognostic performance of the aMTV compared to the cMTV.

## Results

*Patient characteristics*

Overall, 71 of the 280 (25.0%) patients died during the follow-up period (median 54.5 months), resulting in 5- and 10-year OS rates of 81.6% and 53.6%, respectively. The characteristics of the included patients are summarized in Table 1. Briefly, the training group consisted of 66 male and 124 female patients: the validation group was 27 male and 63 female patients. The ages of the patients in the training group ranged from 13 to 84 years (median 64 yrs, IQR 56–70 yrs); those for the patients in the test group were 14–80 years (median 62 yrs, IQR 51.8–69 yrs). There were no significant differences between the training and test groups in age, sex, or distribution of metastatic organs. The range of follow-up periods of the training group was 1.15–154.8 months (median 53.9, IQR 25.2–92.6 mos.) and 2.66–153.1 months (median 56.6, IQR 30.5–95.9 mos.)

for the test group. Among the 71 patients who died during the follow-up period, 51 belonged to the training group and 20 to the test group.

*Univariate analysis*

The results of univariate analysis of organ-based MTVs for OS prediction are summarized in the Table 2. When each organ-based MTV was used as a continuous variable, c-indexes were 0.5454 ($MTV_{neck\text{-}node}$), 0.6046 ($MTV_{distant\text{-}node}$), 0.5708 ($MTV_{lung}$), 0.5252 ($MTV_{bone}$), and 0.5596 ($MTV_{other\text{-}organ}$). We dichotomized these MTVs by using the best cut-off values searched in 0.1-mL steps. The best cut-offs were 2.9 mL for $MTV_{neck\text{-}node}$ (c-index = 0.5841), 0.3 mL for $MTV_{distant\text{-}node}$ (c-index = 0.6026), 1.5 mL for $MTV_{lung}$ (c-index = 0.5784), 15.5 mL for $MTV_{bone}$ (c-index = 0.5419), and 0.1 mL for $MTV_{other\text{-}organs}$ (c-index = 0.5593).

*Multivariate analysis (multivariate model construction)*

We compared the c-indexes between each organ-based MTV's continuous form and its dichotomized form (i.e., without vs. with dichotomization). The form that provided the higher c-index was used for the subsequent multivariate analysis. Based on the results described above, $MTV_{distant\text{-}node}$ and $MTV_{other\text{-}organs}$ as continuous variables and $MTV_{neck\text{-}node}$, $MTV_{lung}$, and $MTV_{bone}$ as dichotomized variables were selected as the input for a multivariate analysis. The estimated weighting coefficients was calculated as 0.69 for dic($MTV_{neck\text{-}node}$), 0.02 for $MTV_{distant\text{-}node}$, 1.05 for dic($MTV_{lung}$), 1.58 for dic($MTV_{bone}$), and 0.01 for $MTV_{other\text{-}organs}$ (Table 3). Note that dic(x) indicates 0 when $x<\theta$ and 1 when $x\geq\theta$ with $\theta$ being the cut-off determined in the univariate analysis.

We thus defined the aMTV (adjusted whole-body MTV) as follows:

$$aMTV = 0.69 \times dic(MTV_{neck\text{-}node}) + 0.02 \times MTV_{distant\text{-}node} + 1.05 \times dic(MTV_{lung}) + 1.58 \times dic(MTV_{bone}) + 0.01 \times MTV_{other\text{-}organs}$$

*Model validation*

Lastly, we evaluated the prognostic performance of the aMTV compared to the cMTV, using the validation dataset. As a result of the univariate analysis to predict OS, the c-index of the aMTV was 0.7676, which was higher than that of the cMTV (0.7218). In the results of the survival analysis with Kaplan-Meier curves using the log-rank test to divide the data into two groups using the median, both aMTV and cMTV were prognostic factors (p=0.0002 and p=0.0006, respectively) (Fig. 3).

The time-dependent ROC analysis to predict 1-year, 3-year, and 5-year survival in the training dataset demonstrated that the aMTV had larger AUCs than the cMTV in the training dataset (Fig. 4). The respective AUC values of the aMTV and cMTV were 0.7436 vs. 0.5169 for 1-year survival, 0.6855 and 0.5687 for 3-year survival, and 0.6553 and 0.5679 for 5-year survival. Similarly, the aMTV produced larger AUC values than the cMTV in the validation dataset (Fig. 5). The respective AUC values of the aMTV and cMTV for the validation dataset were 0.8566 and 0.7846 for 1-year survival, 0.7568 and 0.6528 for 3-year survival, and 0.7867 and 0.6314 for 5-year survival.

## Discussion

We investigated the usefulness of organ-based MTVs over the conventional MTV measured on FDG-PET in patients with DTC. The results can be summarized as follows. (1) The univariate

analysis suggested that $MTV_{distant\text{-}node}$ and $MTV_{other\text{-}organs}$ as continuous variables and $MTV_{neck\text{-}node}$, $MTV_{lung}$, and $MTV_{bone}$ as dichotomized variables were significant prognostic factors. (2) With the multivariate analysis, we estimated weighting factors of each organ-based MTV. (3) Using the weighting factors and the separated test dataset, we observed that the aMTV was superior to the cMTV in terms of predicting the OS of the patients.

Volume-based parameters of FDG-PET/CT, such as MTV and TLG, have been shown to be useful for prognostic factors in various malignant tumors [15–17]. This also applies to thyroid cancer. However, few reports have focused on organ-based MTVs, although it has been reported that the MTV of lung metastasis may be prognostic [18].

To our knowledge, the present study is the first to focus on measuring the MTV of DTC patients in an organ-by-organ manner. This study is also an investigation of the largest number of DTC patients regarding volume-based parameters of FDG-PET.

In clinical practice, we often encounter the following situation: two patients have almost equivalent whole-body MTVs but have different prognoses as their metastatic organs differ. In the relevant literature, metastasis to neck nodes has shown little relevance to prognosis in DTCs, whereas metastatic brain or liver tumors lead to poor prognosis [11–13]. We thus propose that the new indicator, the aMTV, has better prognostic power than the cMTV.

The results of our analyses demonstrated that some of the organ-based MTVs were linearly correlated with the patients' OS while others were more closely correlated after dichotomization. Several possible reasons for these results can be considered. Although it is known that lung metastasis greatly affects the prognosis of thyroid cancer patients, the patients with lung metastasis of DTC often have many small lesions in both lungs. In such cases, the $MTV_{lung}$ tends to be underestimated due to partial volume effects of PET, even though serum sTg

levels, which reflect the total tumor amount, are high. Notably, the present study involved old-generation PET scanners, and the influence of the partial volume effect may thus have been significant. Further investigations are needed to clarify whether the latest PET scanners with improved resolution can improve the predictive value of $MTV_{lung}$.

In contrast, $MTV_{distant\text{-}node}$ and $MTV_{other\text{-}organs}$ as continuous variables were prognostic factors, showing a linear correlation with OS. Unlike lung metastasis, those metastatic lesions tend to be small in number but large in size. Such characteristics may be suitable for measurement with PET.

We observed that cervical lymph node metastasis was poorly correlated with the DTC patients' OS as a continuous variable. This is consistent with past reports that cervical lymph node metastasis was not closely related to the prognosis of DTC [11]. However, we observed that a strong correlation with the OS was obtained when the $MTV_{neck}$ cut-off value was set to 2.9 mL (equivalent to 1.8 cm in diameter), which is a relatively large volume for neck nodes, indicating that even cervical nodes can affect the prognosis when the lesion is large.

There is no gold standard for MTV measurements in DTC. In general, for various tumors, the tumor boundary is often determined using a relative value of 40% of the SUVmax or a fixed value such as SUV≥3.0 as a threshold value. Since we targeted the whole body this time, it was not practical to use a relative value of the SUVmax for many of the lesions in some cases. We thus chose a fixed SUVmax. In the fixed value method, we considered several cut-off candidates (e.g., 2.5, 3.0, and 3.5). Here, when we use values that are smaller than 2.5, much of the background would be included inside the VOI and a considerable amount of manual correction work would be required, which not only takes time but also reduces reproducibility between operators. In contrast, when values that are larger than 3.5 are used, since thyroid cancer is a

302 basically low-accumulation tumor, the low-accumulation lesions could not be picked up in many
303 cases. We therefore used SUV≥3.0 as the threshold value for the empiric evaluation.
304 Prognostic indicators are useful in determining subsequent treatment strategies. In this
305 study, the aMTV was demonstrated to be an excellent prognosis indicator. A large aMTV was
306 associated with poor prognosis. Patients whose aMTV is large may therefore need careful
307 follow-up plus the introduction of aggressive treatment such as surgery to remove as much tumor
308 tissue as possible, external beam radiation therapy, and/or the use of molecular-targeted drugs
309 including TKIs. It may take time and effort to measure the organ-based MTVs at this point in
310 time, but artificial intelligence techniques will eventually make it possible to measure them
311 automatically and quickly.
312 There are several limitations of this study. It was a retrospective analysis enrolling patients
313 treated at a single institution, which inevitably biased the data selection. The prognosis of the
314 patients with thyroid cancer is generally good, but a long-term follow-up observation is required.
315 A prospective study of patients treated at several institutions is thus difficult to carry out,
316 although such a study is important. In addition, we did not investigate our patients' subsequent
317 treatments (further I-131 therapy, external irradiation, surgical dissection, etc.). The imaging
318 devices used for PET also differed among the patients. Although complicated, there is a method
319 of volume measurement that is able to harmonize images with different spatial resolutions; this
320 may be a future research subject. Moreover, although we preliminarily determined the weights of
321 organ-based MTVs, the weights ideally should be determined in as large a population as
322 possible. Finally, there were no confirmations by pathological examinations that metastasis was
323 present.
324

## Conclusion

In patients with DTC with FDG-avid metastasis before I-131 therapy, all organ-based MTVs were significant predictors of patient prognoses. The adjusted whole-body MTV may have the potential to improve the performance of conventional MTV. Measuring the MTV by organ is clinically meaningful.


## Acknowledgments

We thank all staff in the nuclear medicine department of our hospital for their support with the cyclotron operation, radiosynthesis, and image acquisition.

## Funding

This work was supported by a grant from the JSPS KAKENHI, no. JP20K08015.


## Conflict of interest

The authors declare that they do not have anything to disclose regarding funding or conflicts of interest with respect to this manuscript.

## Figure Legends

**Fig. 1.** We retrospectively enrolled 280 patients with DTC who underwent FDG-PET before their initial I-131 therapy after undergoing a total thyroidectomy, and those who had any FDG-avid metastases.

**Fig. 2.** A female patient in her 70s with multiple metastases of thyroid follicular cancer. The metastatic lesions are displayed with different colors for each organ for the measurement of organ-based MTVs.

**Fig.3.** Kaplan-Meier survival curves for the patients in the test group in relation to the aMTV **(a)** and the cMTV **(b)**. Risk stratification was better achieved using the aMTV than the cMTV, up to the sixth year (72 months) after PET scanning.

**Fig. 4.** The training dataset was analyzed with the time-dependent receiver operating characteristic (ROC) curves in predicting (a) 1-year, (b) 3-year, and (c) 5-year survival using the aMTV vs. the cMTV. The AUC was larger for the aMTV than for the cMTV in all of the analyses.

**Fig. 5.** The validation dataset was analyzed with the time-dependent ROC curves in predicting (a) 1-year, (b) 3-year, and (c) 5-year survival using the aMTV vs. the cMTV. The AUC was larger for the aMTV than for the cMTV in all of the analyses.

## References


1. Durante C, Haddy N, Baudin E et al. Long-term outcome of 444 patients with distant metastases from papillary and follicular thyroid carcinoma: Benefits and limits of radioiodine therapy. J Clin Endocrinol Metab. 2006;91:2892-2899.
2. Yang L, Shen W, Sakamoto N. Population-based study evaluating and predicting the probability of death resulting from thyroid cancer and other causes among patients with thyroid cancer. J Clin Oncol. 2013;31:468-474.
3. Yoshio K, Sato S, Okumura Y et al. The local efficacy of I-131 for F-18 FDG PET positive lesions in patients with recurrent or metastatic thyroid carcinomas. Clin Nucl Med. 2011;36:113-117.
4. Gaertner FC, Okamoto S, Shiga T et al. FDG PET performed at thyroid remnant ablation has a higher predictive value for long-term survival of high-risk patients with well-differentiated thyroid cancer than radioiodine uptake. Clin Nucl Med. 2015;40:378-383.
5. Mantziari S, Pomoni A, Prior JO et al. 18 F- FDG PET/CT-derived parameters predict clinical stage and prognosis of esophageal cancer. BMC Med Imaging. 2020 Jan 22;20(1):7.
6. Lovinfosse P, Polus M, Van Daele D, Martinive P et al. FDG PET/CT radiomics for predicting the outcome of locally advanced rectal cancer. Eur J Nucl Med Mol Imaging. 2018 Mar;45(3):365-375.
7. Li Y, Wu X, Huang Y et al. 18 F-FDG PET/CT in lung adenosquamous carcinoma and its correlation with clinicopathological features and prognosis. Ann Nucl Med. 2020 May;34(5):314-321.
8. Wang W, Larson SM, Fazzari M et al. Prognostic value of [18F]fluorodeoxyglucose positron emission tomographic scanning in patients with thyroid cancer. J Clin Endocrinol Metab.

2000;85:1107-1113.

9. Kim BH, Kim S-J, Kim U et al. Diagnostic value of metabolic tumor volume assessed by 18F-FDG PET/CT added to SUVmax for characterization of thyroid 18F-FDG incidentaloma. Nucl Med Commun. 2013;34:868-876.
10. Tam S, Boonsripitayanon M, Amit M et al. Survival in differentiated thyroid cancer: Comparing the AJCC Cancer Staging Seventh and Eighth Editions. Thyroid. 2018;28):1301-1310.
11. Brient C, Mucci S, Taïeb D et al. Differentiated thyroid cancer with liver metastases: Lessons learned from managing a series of 14 patients. Int Surg. 2015;100:490-496.
12. de Figueiredo BH, Godbert Y, Soubeyran I et al. Brain metastases from thyroid carcinoma: A retrospective study of 21 patients. Thyroid. 2014;24:270-276.
13. Collins GS, Reitsma JB, Altman DG et al., members of the TRIPOD group. Transparent Reporting of a Multivariable Prediction Model for Individual Prognosis or Diagnosis (TRIPOD): The TRIPOD Statement. Eur Urol. 2015;67:1142-1151.
14. Hirata K, Kobayashi K, Wong K-P et al. A semi-automated technique determining the liver standardized uptake value reference for tumor delineation in FDG PET-CT. PLOS ONE. 2014;9:e105682.
15. Robbins RJ, Wan Q, Grewal RK et al. Real-time prognosis for metastatic thyroid carcinoma based on 2-[18F]fluoro-2-deoxy-D-glucose-positron emission tomography scanning. J Clin Endocrinol Metab. 2006;91:498-505.
16. Masson-Deshayes S, Schvartz C, Dalban C et al. Prognostic value of (18)F-FDG PET/CT metabolic parameters in metastatic differentiated thyroid cancers. Clin Nucl Med. 2015;40:469-475.

17. Manohar PM, Beesley LJ, Bellile EL et al. Prognostic value of FDG-PET/CT metabolic parameters in metastatic radioiodine-refractory differentiated thyroid cancer. Clin Nucl Med. 2018;43:641-647.
18. Maruoka Y, Baba S, Isoda T, Kitamura Y, Abe K, Sasaki M, Honda H. Association between volumetric analysis of lung metastases on F-18-fluoro-2-deoxy-D-glucose positron emission tomography/computed tomography and short-term progression after I-131 therapy for differentiated thyroid carcinoma. Indian J Nucl Med. 2017;32(3):167-172.

Table 1. Characteristics of the 280 patients included in the study.

| | Training | Test | p -value |
|---|---|---|---|
| **Number of patients** | 190 | 90 | |
| **Gender** | | | |
| male | 66 | 27 | 0.4282 |
| female | 124 | 63 | |
| **Age** | | | |
| range | 13-84 | 14-80 | 0.573 |
| (median, IQR) | (61.1, 56-70) | (60.0, 51.8-69) | |
| **Pathology** | | | |
| papillary | 149 (78.4%) | 80 (88.9%) | 0.1661 |
| follicular | 23 (12.1%) | 4 (4.4%) | |
| poor | 15 (7.9%) | 5 (5.6%) | |
| papillary + follicular | 3 (1.6%) | 1 (1.1%) | |
| **Metastatic site** | | | |
| neck lymph node | 149 (78.4%) | 72 (80.0%) | 0.7632 |
| distant lymph node | 44 (23.2%) | 25 (27.8%) | 0.404 |
| lung | 95 (50.0%) | 46 (51.1%) | 0.8627 |
| bone | 30 (15.8%) | 10 (11.1%) | 0.2978 |
| others | 7 (3.7%) | 3 (3.3%) | 0.8831 |
| **Follow up period** | | | |
| range | 1.15-154.8 | 2.66-153.1 | 0.4042 |
| (median, IQR) | (53.9, 25.2-92.6) | (56.6, 30.5-95.9) | |
| **Outcome** | | | |
| dead | 51 (26.8%) | 20(22.2%) | 0.4084 |
| alive | 154 (73.2%) | 74(77.8%) | |
| **PET scanner** | | | |
| EXACT47 | 95 (50.0%) | 43 (47.8%) | 0.8756 |
| Biograph | 85 (44.7%) | 43 (47.8%) | |
| HR+ | 10 (5.3%) | 4 (4.4%) | |

Table 2. Univariate analysis

| | Continuous value | | | Dichotomized value | | | |
|---|---|---|---|---|---|---|---|
| | p-value | Hazard ratio | 95%CI | Cut-off | p-value | Hazard ratio | 95%CI |
| $MTV_{neck\text{-}node}$ | 0.0763 | 1.016 | [-0.0021, 0.028] | 2.9 | 0.0258 | 2.004 | [0.52, 1.84] |
| $MTV_{distant\text{-}node}$ | 0.0997 | 1.015 | [-0.0038, 0.027] | 0.3 | 0.0003 | 3.345 | [0.58, 1.78] |
| $MTV_{lung}$ | 0.3059 | 1.002 | [-0.0036, 0.0043] | 1.5 | 0.0082 | 2.390 | [0.23, 1.45] |
| $MTV_{bone}$ | 0.0060 | 1.014 | [0.0048, 0.021] | 15.5 | 0.0062 | 3.430 | [0.39, 1.96] |
| $MTV_{other\text{-}organs}$ | 0.0011 | 1.012 | [0.0057, 0.017] | 0.1 | 0.0002 | 10.771 | [1.28, 3.27] |

Table 3. Multivariate analysis

| | p-value | Regression coefficient | Hazard ratio | 95%CI |
|---|---|---|---|---|
| $d(MTV_{neck\ node})$ | 0.308 | 0.69 | 2.096 | [-0.681, 2.161] |
| $MTV_{distant\ node}$ | 0.018 | 0.02 | 1.039 | [0.007, 0.070] |
| $d(MTV_{lung})$ | 0.002 | 1.05 | 7.084 | [0.694, 3.222] |
| $d(MTV_{bone})$ | 0.065 | 1.58 | 7.560 | [-0.128, 4.174] |
| $MTV_{other\text{-}organs}$ | 0.669 | 0.01 | 0.999 | [-0.008, 0.005] |

**Fig. 1**

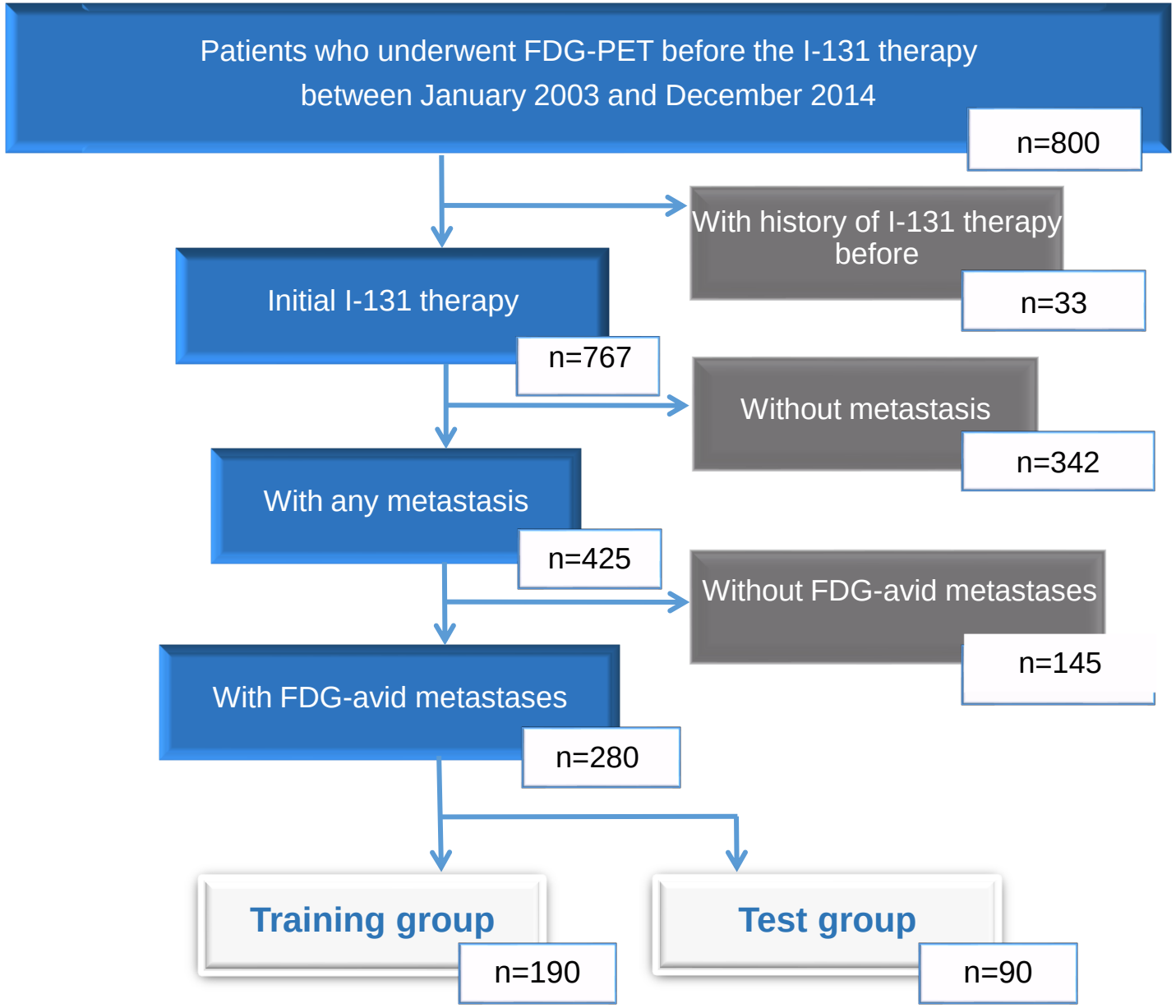
Patients who underwent FDG-PET before the I-131 therapy between January 2003 and December 2014
n=800
With history of I-131 therapy before
n=33
Initial I-131 therapy
n=767
Without metastasis
n=342
With any metastasis
n=425
Without FDG-avid metastases
n=145
With FDG-avid metastases
n=280
Training group
n=190
Test group
n=90

**Fig. 2**

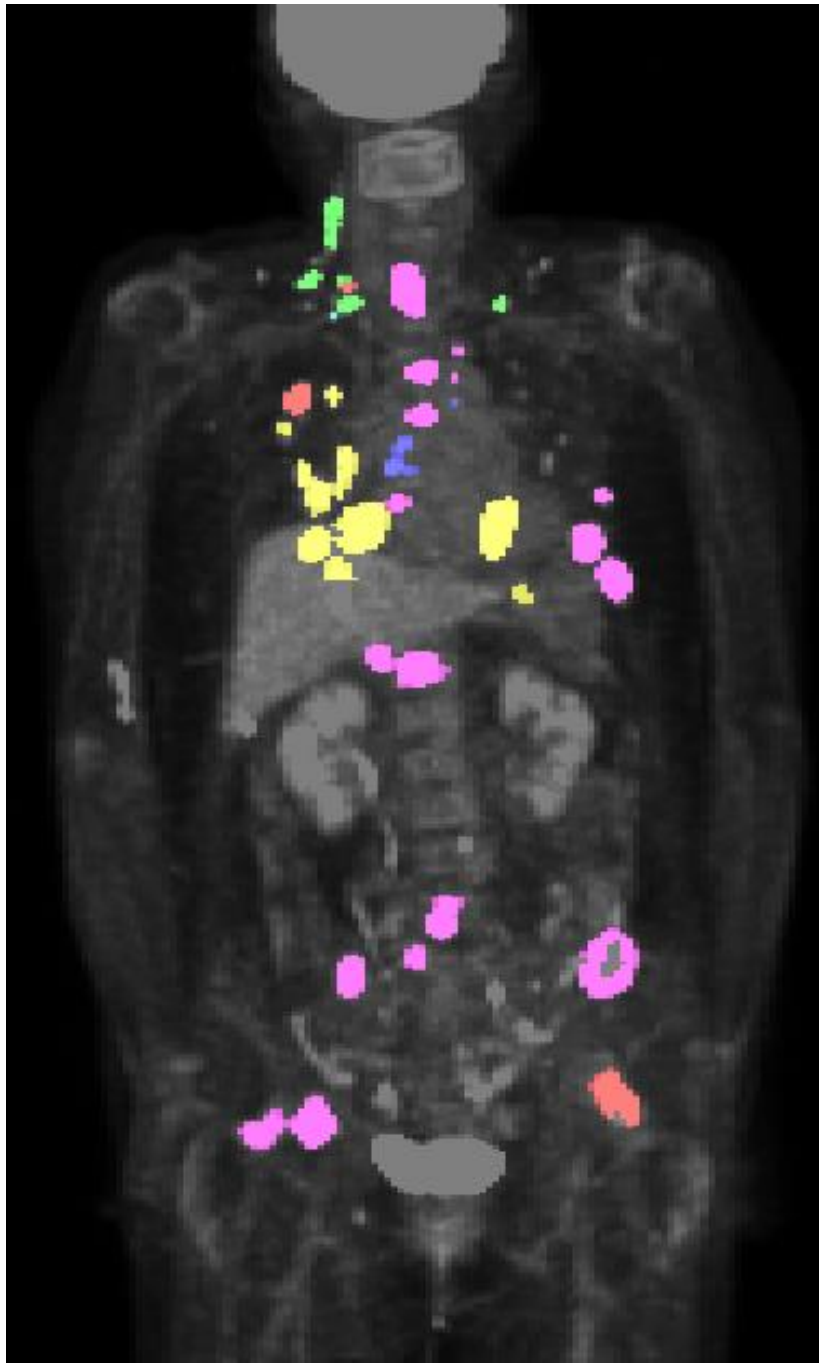

Neck node
Distant node
Lung
Bone
Others

| Region | MTV (mL) |
|---|---|
| Neck node | 7.331 |
| Distant node | 2.992 |
| Lung | 52.283 |
| Bone | 134.629 |
| Others | 17.451 |
| All | 214.686 |

# Fig. 3

a

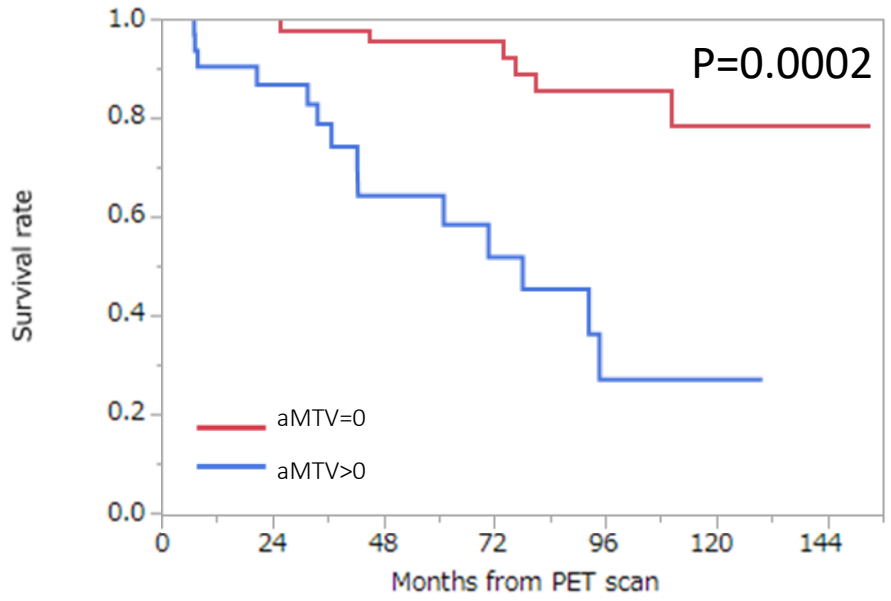


| | | | | | | | |
|---|---|---|---|---|---|---|---|
| Total o. of patients | 90 | 74 | 53 | 39 | 24 | 13 | 2 |
| aMTV=0 | 58 | 49 | 40 | 30 | 21 | 11 | 2 |
| aMTV>0 | 32 | 25 | 13 | 9 | 3 | 2 | 0 |

b

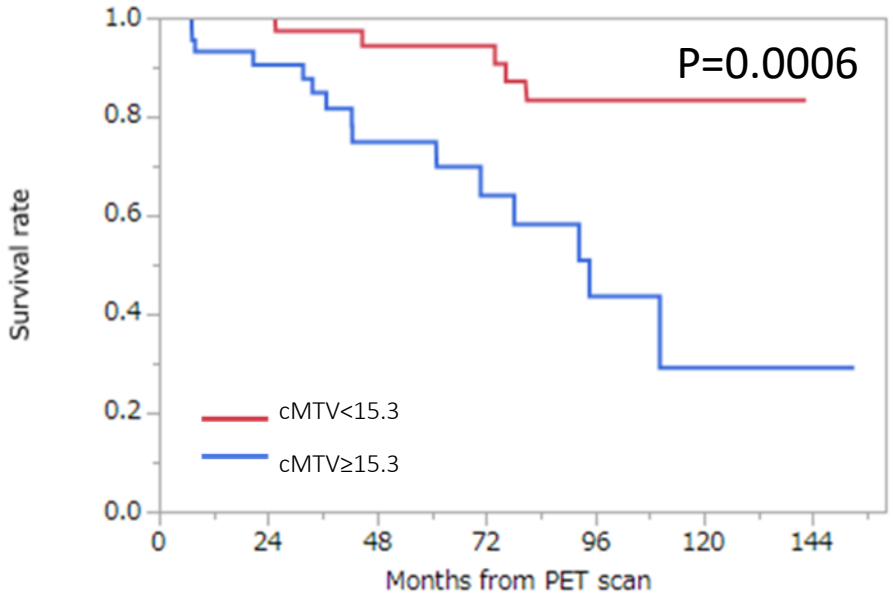


| | | | | | | | |
|---|---|---|---|---|---|---|---|
| Total o. of patients | 90 | 74 | 53 | 39 | 24 | 13 | 2 |
| cMTV<15.3 | 45 | 39 | 31 | 27 | 18 | 10 | 1 |
| cMTV≥15.3 | 35 | 35 | 22 | 12 | 6 | 3 | 1 |

# Fig. 4

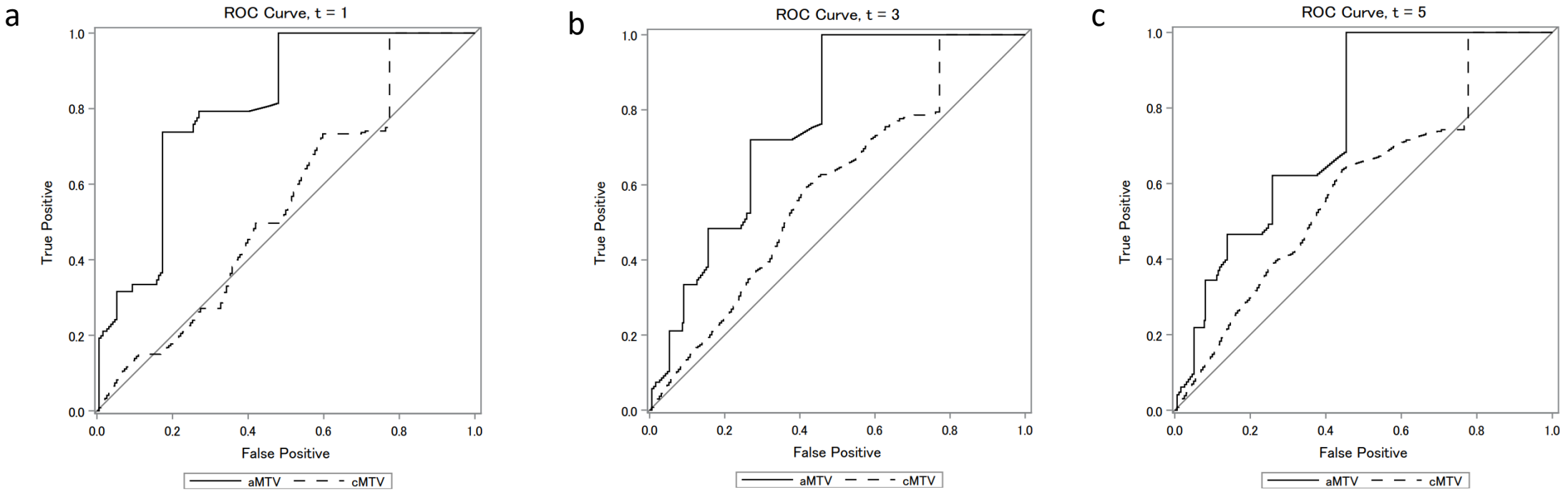
a
ROC Curve, t = 1
True Positive
False Positive
0.0
0.2
0.4
0.6
0.8
1.0
aMTV
cMTV
b
ROC Curve, t = 3
True Positive
False Positive
aMTV
cMTV
c
ROC Curve, t = 5
True Positive
False Positive
aMTV
cMTV

# Fig. 5

a

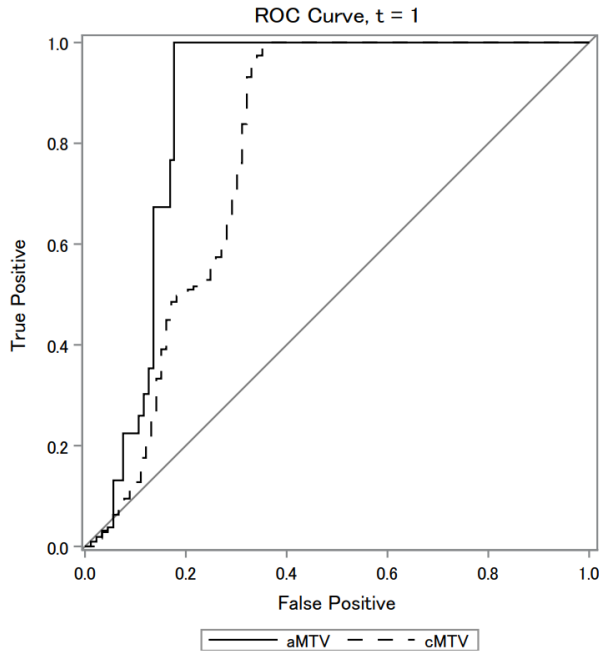
ROC Curve, t = 1
True Positive
False Positive
0.0
0.2
0.4
0.6
0.8
1.0
aMTV
cMTV

b

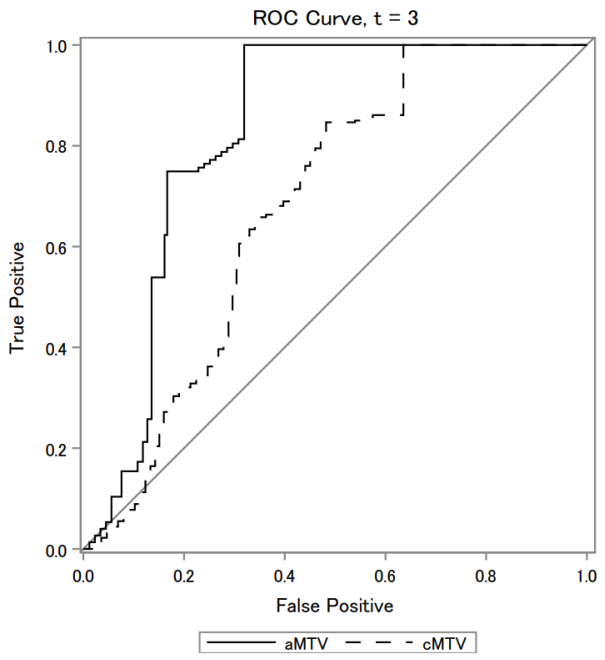
ROC Curve, t = 3
True Positive
False Positive
0.0
0.2
0.4
0.6
0.8
1.0
aMTV
cMTV

c

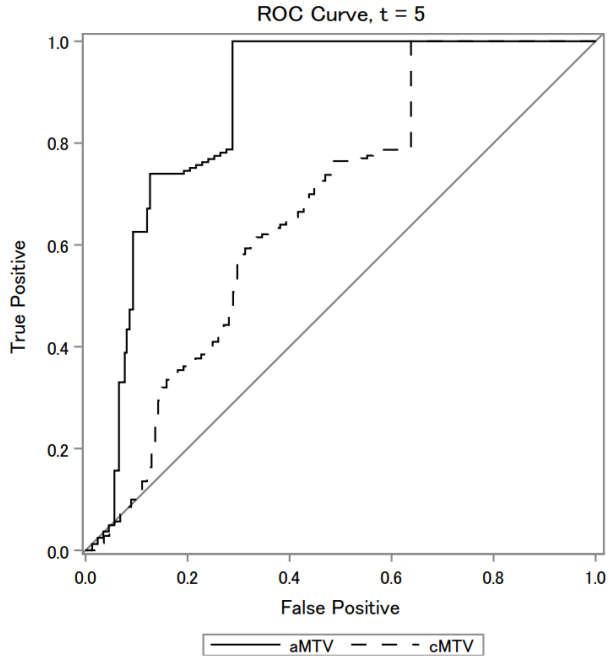
ROC Curve, t = 5
True Positive
False Positive
0.0
0.2
0.4
0.6
0.8
1.0
aMTV
cMTV